# Characterisation and Comparison of Diamond-Like Carbon Thin Films Deposited by RF-PECVD and Pulsed-DC Hollow Cathode PECVD

*I.A. Birney*, F. Placido, and J. Kavanagh,*
*Thin Film Centre, University of the West of Scotland, Paisley, United Kingdom*

**I.A. Birney author name updated from original manuscript on February 23, 2024; no other changes to original document.*

## ABSTRACT

A considerable amount of research has taken place into diamond-like carbons (DLCs) in the years since they were first described over 30 years ago. DLCs have since found a wide range of applications, including in optoelectronic devices, solar cells, infrared optics, and as a protective coating for metals in corrosive and/or abrasive environments. These consist of the amorphous hydrogen-carbon alloys (a-C:H), hydrogen-free amorphous carbons (a-C) and tetrahedrally-structured amorphous carbons, (ta-C), which can contain in excess of 90% $sp^3$ bonding. In this paper, diamond-like carbon thin films have been deposited on silicon wafer and fused silica substrates by two distinct methods; radio frequency (RF) plasma-enhanced chemical vapour deposition (PECVD), and pulsed-DC hollow cathode PECVD, using hydrocarbon precursors. The resultant DLC films fabricated via these two methods have been characterized and compared using several methods; the optical properties of these films have been modelled and measured using transmittance/reflectance spectroscopy; the physical properties of these films have also been examined, by nanoindentation, surface energy measurement, and the nanostructure of the films studied by scanning electron microscopy (SEM) and atomic force microscopy (AFM).

## INTRODUCTION

Diamond-like carbon (DLC) is a metastable form of amorphous carbon, comprising a network of tetrahedrally- ($sp^3$ hybridized) and trigonally- ($sp^2$ hybridized) bonded carbon atoms. In addition to this, DLC films often contain a significant proportion of hydrogen, both bound and unbound, within the matrix. DLC has attracted a great deal of interest since interest since it was first synthesised and described by Aisenberg and Chabot [1, 2].

Within the DLC film matrix, the bonding can range from being completely graphitic in character (100% $sp^2$) to being very similar to that of diamond; the latter is usually referred to in the literature as tetrahedral amorphous carbon (ta-C) and can have up to 90 % $sp^2$ bonding [3].

However, usage of the term 'DLC' can also refer to the hydrogen-free amorphous carbons (a-C), and the amorphous carbon-hydrogen alloys (a-C:H) [2,3,4]. DLC films of these types can contain anywhere from 1 % to 50 % hydrogen, with a-C:H generally containing less than 50 % $sp^3$ fraction and a-C generally containing 85 % or more $sp^3$ bonding [5, 6]. (It is worthy of note, however, that in addition to carbon-carbon DLC bonds, carbon-hydrogen bonds can also be in the $sp^3$ configuration. Thus, increased hydrogen content can increase the $sp^3$ content )

It is generally accepted that many of the attractive properties of DLC are conferred by the $sp^3$ carbon-to-carbon bonds, such as the high density and compact structure, the high level of hardness and wear resistance. Although the addition of C-H $sp^3$ bonds also promotes a tetrahedral structure, these have a detrimental effect on the mechanical properties of the film. (They also have an effect on the optical and electronic properties of the matrix, due to the increase in the quantity of $\sigma$-electrons and decrease in the quantity of $\pi$-electrons) [4].

DLCs are currently utilized in a wide variety of applications, including in optoelectronic devices [7], solar cells, infrared optics [8], as an impermeable gas barrier inside PET drinks bottles [9] and as a protective coating for metals in corrosive and/or abrasive environments [10, 11].

In this paper, the characterization of a-C:H type DLC films prepared by both RF-PECVD and HC-PECVD, is discussed, and the resultant films produced by each of the two methods are compared.

## EXPERIMENTAL DETAILS

Films were deposited on both silicon <100> wafer and fused silica glass substrates, both by RF-PECVD and by hollow cathode pulsed-DC PECVD. A schematic of the RF-PECVD deposition apparatus is shown on the left hand side of Figure 1; and a schematic of the pulsed-DC PECVD apparatus on the right hand side.

 505/856-7188

54th Annual Technical Conference Proceedings, Chicago, IL April 16–21, 2011 ISSN 0737-5921

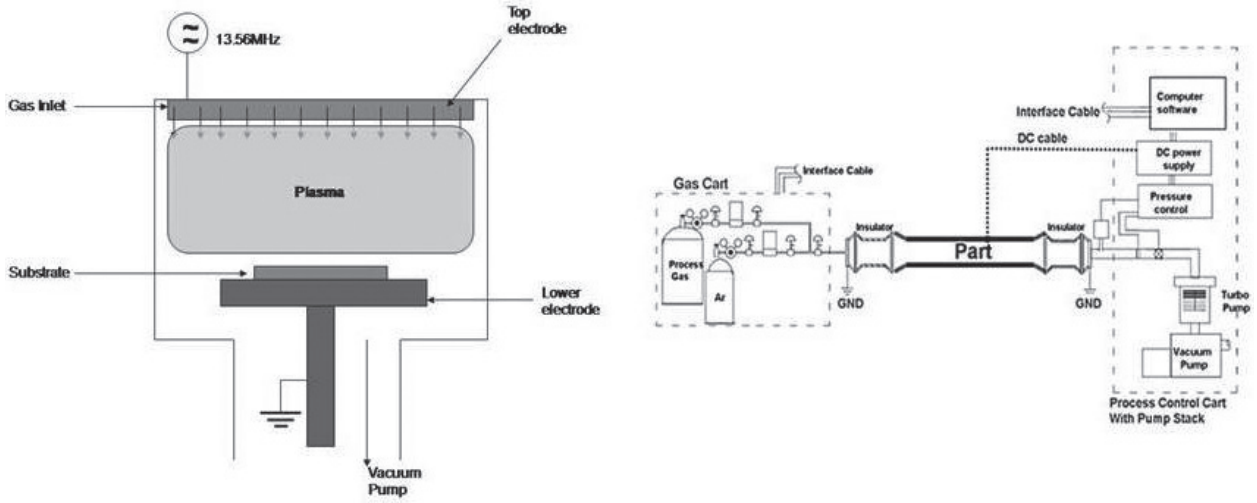


*Figure 1: Left: Schematic of PECVD apparatus; Right: Schematic of hollow cathode pulsed-DC PECVD apparatus [10].*

All substrates were cleaned prior to deposition with isopropanol and then argon etched. For the standard RF-PECVD depositions, conditions were 10 minutes' deposition time at each of 200W, 400W and 600W forward power, at 30 mTorr chamber pressure, with 15 sccm and 25 sccm flow rates of argon and acetylene respectively. For the pulsed-DC hollow cathode PECVD depositions, conditions were also 10 minutes' deposition time at each of 200W, 400W and 600W cathode power, and 20W, 35W and 50W anode power respectively, with flow rates of 90 sccm and 130 sscm of argon and acetylene respectively, at a deposition pressure of 120 mTorr .

The structure of the films were examined using a Digital Instruments' NanoScope III atomic force microscope (AFM) in contact mode, with silicon nitride cantilever. The scan size was 10μm$^2$. Films were also examined and imaged in a Hitachi S-2000 scanning electron microscope (SEM).

The contact angles and surface energy of the DLC films were measured using a KSV Instruments' CAM200 contact angle goniometer and SFECAM software. Three solvents of known surface tension components; namely deionised water, diiodomethane and ethylene glycol; were used to enable calculation of surface free energy, using the Fowkes/ Owens-Wendt-Kaelble equation:

$$\gamma_{lv}(1+\cos\theta) = 2\sqrt{\gamma_{sv}^{d}\gamma_{lv}^{d}} + 2\sqrt{\gamma_{sv}^{p}\gamma_{lv}^{p}} \qquad (1)$$

Where $\gamma_{lv}$ is liquid-vapour interfacial energy, $\gamma_{sv}$ is solid-vapour interfacial energy, and *d* the and $\rho$ superscripts denote dispersive and polar components of the interfacial energies respectively.

Thus, at least two measurements with different solvents, of known dispersive and polar surface tension components, are required in order to solve the system of equations and in doing so, to calculate the surface energy of the solid phase. This approach to the calculation of surface energy is discussed at length elsewhere [12, 13].

The hardness and reduced modulus of the DLC samples deposited on silicon wafer substrate were measured using a Hysitron TriboScope nano-indenter system with a three-sided pyramid (Berkovich) diamond tip. In this method, a small diamond-tipped probe is forced into the film progressively, and the force-displacement curve is plotted. The curve is also measured during the unloading cycle. The pressure under the diamond tip, calculated from the ratio of force to the area of plastic deformation, defines the hardness. The unloading curve is used to calculate the reduced modulus, by drawing the tangent from the maximum load point and extrapolating backward to zero load. The Young's modulus and hardness can thus be calculated. The maximum load force used in the nanoindentation measurements was 5000 μN.

The transmission and reflection spectra of the DLC films, deposited on silica glass substrates at 400W power, were measured using an Aquila Instruments' nkd-8000 spectrometer with Pro-Optix software. Samples were examined in S-polarized light at 10º angle of incidence, both in transmission and reflection, over the 350-1100 nm wavelength range. The data were fitted using a Cauchy model, enabling calculation of film thickness as well as refractive index and extinction coefficient.

## RESULTS AND DISCUSSION

### Structure and Hardness

Figure 2 shows the hardness and reduced modulus values of the films deposited with varying power, by both deposition methods, and measured by nano-indentation. In the case of RF-PECVD films, there seems to be a general upward hardness trend with increasing deposition power; this is less obvious in the case of HC-PECVD films. In the case of the RF-PECVD films, the values for hardness and reduced modulus, ranging from approximately 14-17 GPa and 128-133 GPa respectively, are consistent with those reported elsewhere for a-C:H type films [2, 5]. In the case of the HC-PECVD films, the measured values for hardness and reduced modulus were lower than this, ranging from approximately 10-12 GPa and 78-96 GPa respectively.

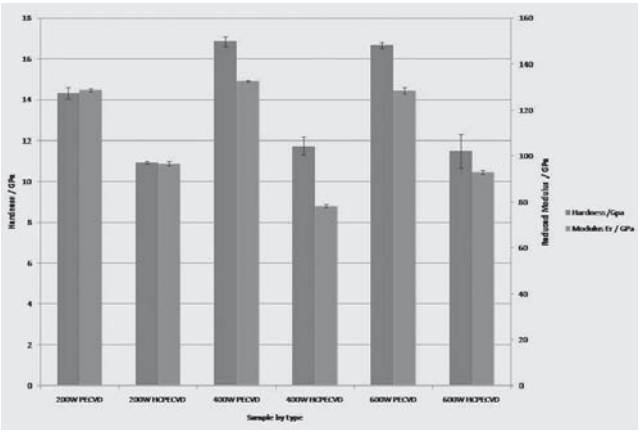


*Figure 2: Graph showing the values of hardness and reduced modulus, $E_R$, for the film samples prepared with varying by each of the two methods, with varying deposition power.*

The films were imaged by AFM, with a scan size of 10 $\mu m^2$. An example of the images captured is shown in Figure 3. The average roughness of the samples produced by HC-PECVD was somewhat larger than that of the PECVD samples. This can be partly explained by the fact that average roughness $R_a$ generally increases with increasing film thickness, and that the HC-PECVD samples were considerably thicker than the PECVD samples.

In addition to the AFM imaging, the samples were examined by SEM. The surface of each of the HC-PECVD samples also appeared to be rougher than those of the PECVD samples, as shown by example in Figure 4. In addition, the thickness of the HC-PECVD samples was considerably higher than those of the PECVD samples; Table 1 shows the film thicknesses of the samples as deposited on silicon wafer and determined by cross-sectional SEM, in addition to the thicknesses of samples deposited on fused silica and calculated by optical measurement and modelling.

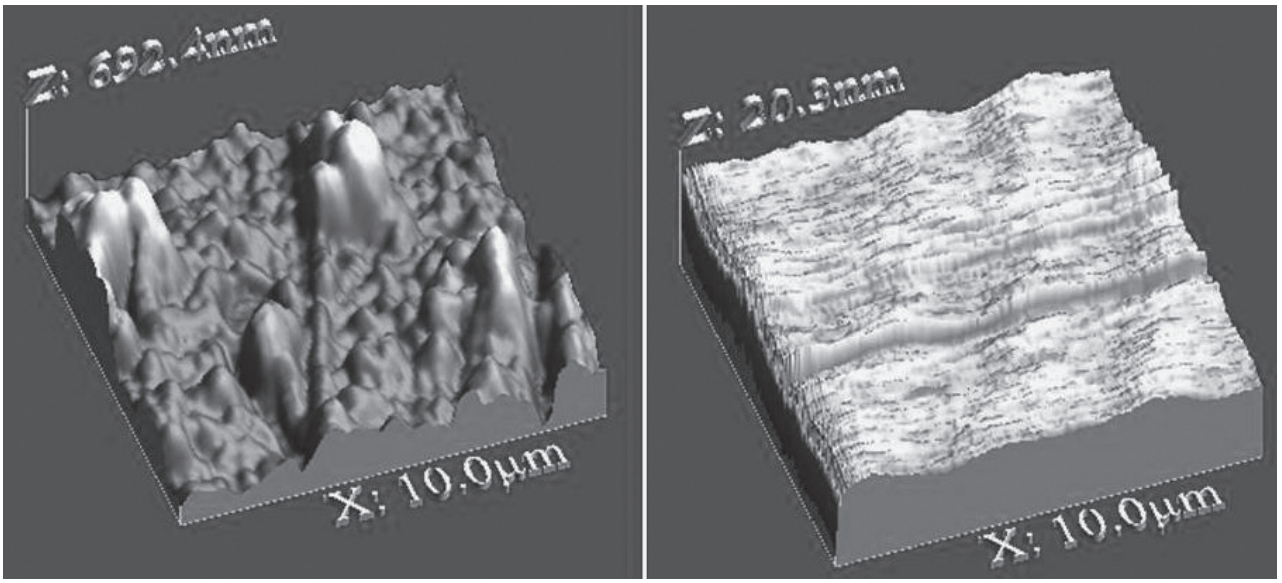


*Figure 3: Example AFM images. The leftmost image shows the surface of DLC produced by HCPECVD on silicon substrate at 400W forward power; the rightmost image depicts the surface of PECVD-produced DLC on silicon, also at 400W forward power.*

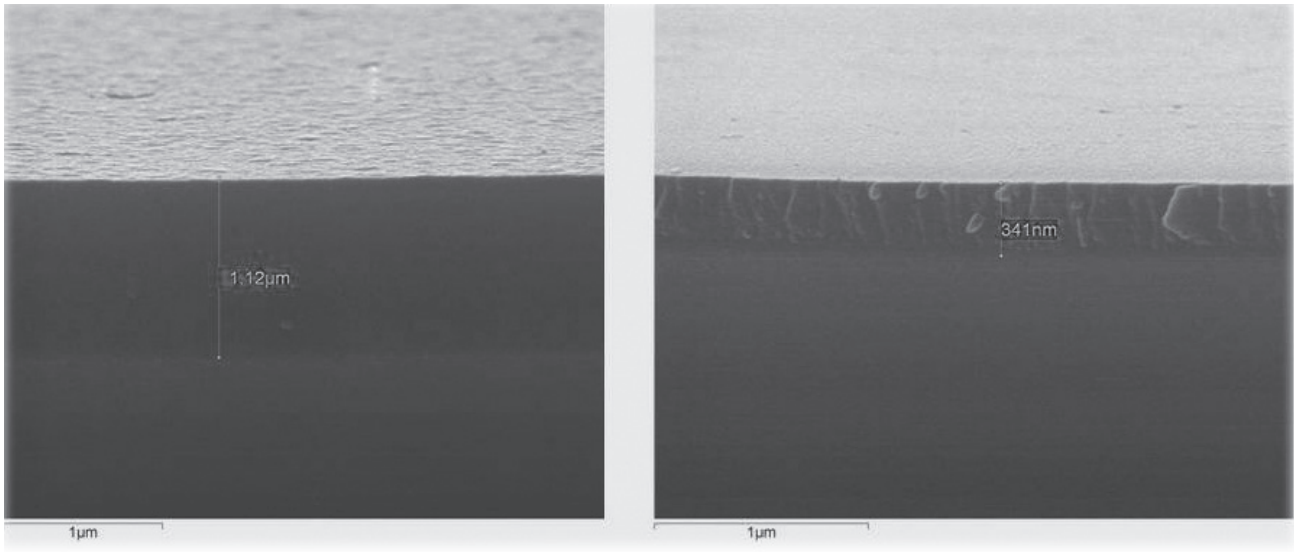


*Figure 4: SEM images of (left) DLC deposited on silicon at by HCPECVD at 400W power, and (right) DLC deposited on silicon at 400W power, both over a 10 minute deposition period. Note the rougher surface of the HCPECVD sample, and the greater film thickness.*

*Table 1: Film thicknesses determined by cross-sectional SEM of the samples as deposited on silicon wafer and optical measurement and modelling on samples as deposited on fused silica.*

| DLC sample | Mean thickness/ nm (SEM) | Thickness/nm (Optical measurement) |
|---|---|---|
| PECVD 200W | 228 | - |
| HCPECVD 200W | 505 | - |
| PECVD 400W | 298 | 364 |
| HCPECVD 400W | 1084 | 1626 |
| PECVD 600W | 353 | - |
| HCPECVD 600W | 1040 | - |

The disparity between the thicknesses measured by SEM and transmission/reflection spectra can be explained by the fact that these samples were prepared on different substrates; SEM samples on silicon wafer and optical samples on fused silica. As DLC growth is a sub-surface process, the choice of substrate affects the film growth rate.

In the case of PECVD deposition under these conditions, film growth rate increases with increasing forward power. For the HC-PECVD samples, generally, a higher cathode power would also appear to be linked to increased film growth rate, although there is not a great deal of difference between the 400W and 600W experiments in terms of thickness. (Some variation of film thickness across each of the samples was observed by SEM, showing a degree of non-uniformity.)

## SURFACE ENERGY/CONTACT ANGLE

DLC is noted for its low surface energy [2]. Figure 5 shows the calculated surface free energy (SFE) of the films deposited with varying power, by both deposition methods. There is a general upward trend in terms of surface energy with respect to increasing power for both deposition methods. For the 200W and 400W samples, the PECVD samples have a higher SFE value than the corresponding HC-PECVD samples; however, this is not true of the 600W samples. The values for the PECVD samples fall within the range 41-43 $mNm^{-1}$, and those for the HC-PECVD samples within the range 39-44 $mNm^{-1}$, both of which are consistent with values expected for a-C:H-type DLC [2].

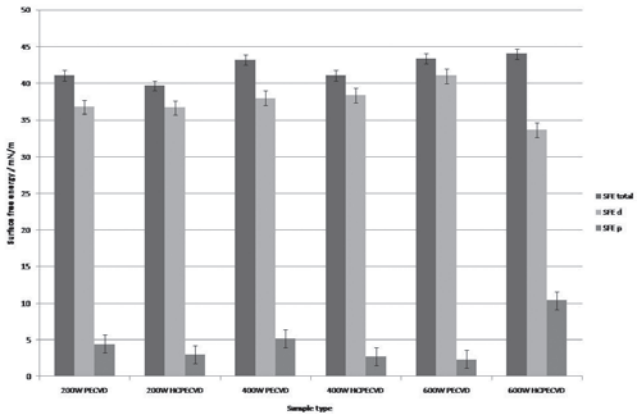


*Figure 5: Graph showing the calculated values of total surface free energy and the separation into its polar and dispersive components, for film samples prepared with varying power, by both deposition methods.*

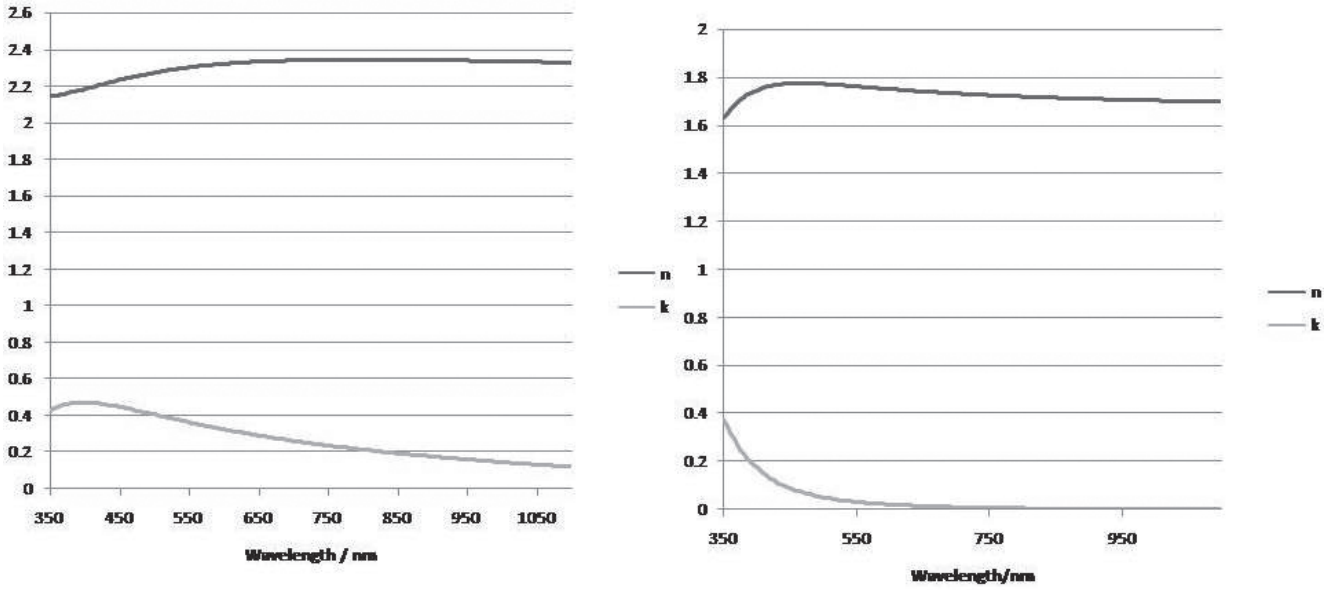


*Figure 6: Refractive index, n and extinction coefficient, k, of samples prepared on fused silica substrate by PECVD (left), and HCPECVD (right), as a function of incident wavelength, calculated from transmission and reflection data.*

**Optical Measurements**

Figure 6 shows the refractive index *n*, and extinction coefficient *k*, of samples prepared on fused silica substrate by both deposition methods, as calculated from the transmission and reflection data using a simple Cauchy model. Both *n* and *k* are somewhat lower for the HC-PECVD sample than for the PECVD sample across the wavelength range examined. The model also enabled calculation of film thickness, as detailed in Table 1, again clearly showing the considerably higher film growth rate of the HC-PECVD method as compared to PECVD.

The *n* and *k* values for the HC-PECVD DLC are lower than those that might typically be measured for DLC films, and could indicate a film high in graphitic/polymeric character, which is consistent with the lower hardness of such samples compared to the corresponding PECVD DLC samples.

**CONCLUSIONS**

A series of a-C:H-type DLC films were synthesized on silicon and silica substrates, at forward power/cathode power of 200W, 400W and 600W, using standard RF-PECVD and pulsed-DC hollow cathode PECVD.

In terms of mechanical properties, a general upward trend in hardness is evident in the PECVD samples with hardness trend with increasing deposition power; but this is less apparent of HC-PECVD films. The values measured are consistent with those reported elsewhere. The PECVD samples exhibited higher hardness and modulus than the corresponding HC-PECVD samples.

In most cases, SFE values are slightly lower for HC-PECVD samples than for PECVD, although this is not true of the 600W power depositions.

Film growth rate is shown to be upwardly increased by increasing deposition power in the case of the PECVD process, although this is less obvious in the case of HC-PECVD. It is clear that the pulsed-DC HC-PECVD film growth process is significantly faster than that of the PECVD process, which, over a 10 minute deposition, results in films that are considerably thicker and rougher than those produced by PECVD. A clear advantage of the HC-PECVD process is that it is possible to deposit quite thick DLC films without sample delamination due to intrinsic stress; previous experiments have shown that the PECVD process is more limited in this respect, with delamination occurring at thicknesses approaching 1µm.

The optical properties of films produced by the two processes are quite markedly different, with *n* and *k* values being lower for the HC-PECVD sample than the PECVD. This is strongly indicative of differences in the bonding in the films produced by the two processes, which will be further examined in future.

**REFERENCES**


1. S.Aisenberg, R.Chabot, "Ion-Beam Deposition of Thin Films of Diamondlike Carbon", J. Appl. Phys. 42 (1971) 2953.

2. J.Robertson, "Diamond-like amorphous carbon", Mat. Sci. Eng. R. 37 (2002) 129.

3. Y.Lifshitz, "Pitfalls in amorphous carbon studies", Diamond Rel. Mater. 12 (2003) 13.

4. Y.Lifshitz, "Diamond-like carbon – present status", Diamond Rel. Mater. 8 (1999) 1659.

5. A.Grill, "Diamond-like carbon: state of the art", Diamond Rel. Mater. 8 (1999) 428.

6. A.Grill, "Electrical and optical properties of diamond-like carbon", Thin Solid Films 355-356 (1999) 189.

7. A.M.M.Omer, Sudip Adhikari, Sunil Adhikari, M.Rusop, H.Uchida, T.Soga, M.Umeno, "Electrical Conductivity improvement by iodine doping for diamond-like carbon thin-films deposited by microwave surface plasma CVD", Diamond Rel. Mater. 15 (2006) 645.

8. X.Bian, Q.Chen, Y.Zhang, L.Sang, W.Tang, "Deposition of nano-diamond-like carbon films by an atmospheric pressure plasma gun and diagnostic by optical emission spectrum on the process", Surf. Coat. Tech. 202 (2008) 5383.

9. A.Ueda, M.Nakachi, S.Goto, H.Yamakoshi, A.Shirakura, "High Speed and High Gas Barrier Rotary DLC Plasma Coating System for PET bottles", Mitsubishi Heavy Industries Ltd., Technical Review 42 (2005) 1.

10. D.Lusk, M.Gore, W. Boardman, T.Casserly, K.Boinapally, M.Oppus, D.Upadhyaya, A. Tudhope, M. Gupta, Y.Cao, S.Lapp, "Thick DLC films deposited by PECVD on the internal surface of cylindrical substrates", Diamond Rel. Mater. 17 (2008) 1613.

11. R.Sharma, P.K.Barhai, N.Kumari, "Corrosion resistant behaviour of DLC films", Thin Solid Films 516 (2008) 539.

12. D.Y.Kwok. A.W.Neumann, "Contact angle measurement and contact angle interpretation", Adv. Colloid Interface Sci. 81 (1999) 202-203.

13. M.Grischke, A.Hieke, F.Morganweck, H.Dimigen, "Variation of the wettability of DLC-coatings by network modification using silicon and oxygen", Diamond Rel. Mater. 7 (1998) 454.